

Annexin I and Annexin II N-Terminal Peptides Binding to S100 Protein Family Members: Specificity and Thermodynamic Characterization[†]

Werner W. Streicher,^{‡,§} Maria M. Lopez,[§] and George I. Makhatadze^{*,‡,§,||}

Department of Biology and Center for Biotechnology and Interdisciplinary Studies, Rensselaer Polytechnic Institute, Troy, New York 12180, and Department of Chemistry and Chemical Biology, Rensselaer Polytechnic Institute, Troy, New York 12180

Received October 25, 2008; Revised Manuscript Received January 21, 2009

ABSTRACT: The S100 proteins make up a family of dimeric calcium binding proteins that function in response to changing calcium levels. Several S100 binding proteins have been identified; however, the exact biological functions of the S100 proteins are largely unknown as there are several factors which modulate their functions. To address these issues, the specificity of binding of representative members of the human S100 proteins to short N-terminal peptides of annexin I (AnI) and annexin II (AnII) was investigated under controlled experimental conditions. AnI and AnII have been shown previously to interact with S100A11 and S100A10, respectively. This provided a unique opportunity to determine their binding specificity with the other members of the human S100 protein family. It was found that AnI binds S100A6 or S100A11 while AnII binds S100A10 or S100A11. This is the first report of the interaction between S100A6 and AnI. The fact that AnI and AnII bind to selected members of the S100 protein family shows that these interactions are specific and that the mode of binding is different from that of calmodulin, as it was found not to bind AnI or AnII. From the analysis of the thermodynamics of interactions, the binding seems to be entropically driven. It was found that both AnI and AnII undergo a coil-to-helix transition upon binding to their respective binding partners. The observation that there is an overlap in functionality is not surprising due to considerable sequence homology between S100 protein family members. In fact, the functional overlap can explain previous failures of S100 knockout constructs to show any detectable changes in phenotype despite numerous implications of these proteins in important cellular processes.

The S100 protein family has attracted significant interest due to their role in responding to changing calcium levels in the cell (for reviews, see refs 1–5). These proteins have been implicated to play roles in the regulation of several key cellular processes ranging from cytoskeleton dynamics to apoptosis (6, 7). However, the understanding of the biological role of S100 proteins is far from comprehensive. In part, this is a result of the possible overlap in their function, which makes traditional approaches such as gene knockout ineffective.

The proteins of the S100 family generally exist as homodimers, with two EF-hand calcium binding motifs per monomer (1). Upon calcium binding, S100 proteins undergo a conformational change which exposes a region on the surface of the protein which has been shown to be responsible for binding several target proteins or peptides (1, 8). There have been several reports on identifying proteins which interact with the S100 proteins providing some insight into their function (for a review, see ref 1). It is generally suggested that the interactions between S100 proteins and

their target proteins are specific due to observations that only certain members of the S100 protein family were found to interact with specific target proteins. However, in many cases, these observations are based mainly on interactions screened for under cellular environments which are difficult to define and control. This makes it difficult to identify additional S100 members which might also interact with the target protein, as only the interacting partners with the highest affinity will be identified. In addition, there are several other factors that can modulate the function of the S100 proteins. These include changing calcium levels in the cells, the presence of other divalent cations, such as zinc and copper, which have been shown to bind at positions distant from the calcium binding site (for a review, see ref 9), tissue specific expression of certain members of the S100 family (10), and post-translational modification of target proteins (8).

For some of the interactions between the S100 proteins and their target proteins, relatively short peptide regions of the target protein have been found to retain the ability to bind the S100 target protein (for example, see refs 11 and 12). Several crystal structures of the S100–peptide complexes have shown that these peptides all bind in the same region which is generally exposed upon calcium binding (13–15).

The fact that short peptides retain the ability to bind S100 proteins provides a unique opportunity to determine whether the S100 proteins can discriminately bind these peptides,

[†] This work was supported in part by a grant from the National Institutes of Health (GM54537).

* To whom correspondence should be addressed: CBIS 3244A, Rensselaer Polytechnic Institute, 110 8th St., Troy, NY 12180. Phone: (518) 276-4417. Fax: (518) 276-2955. E-mail: makhag@rpi.edu.

[‡] Department of Biology.

[§] Center for Biotechnology and Interdisciplinary Studies.

^{||} Department of Chemistry and Chemical Biology.

which would allow for further insight into the degree of S100 specificity and thus their functions. The question of binding specificity is highlighted by the interaction of S100A10 with an N-terminal peptide of the annexin II protein (AnII), and the interaction of S100A11 with the N-terminal peptide of the annexin I protein (AnI). It was initially shown that these binding partners do not exhibit cross reactivity; i.e., S100A10 binds AnII but not AnI, and S100A11 binds AnI but not AnII (15). However, in a more recent study (16), it was suggested that S100A11 does exhibit cross reactivity as it was shown to interact with AnII. Even though these interactions might be specific in the case of S100A10 and S100A11, could these short peptides bind to any of the other members of the S100 protein family? To address this question, 16 members of the human S100 proteins, which represent a pool of biologically relevant variants, and calmodulin were screened for binding with AnI and AnII using several biophysical methods.

MATERIALS AND METHODS

Peptide Purification. Annexin I peptide (AnI; amino acid sequence of Ac-AMVSEFLKQAWFIE) and annexin II peptide (AnII; amino acid sequence of Ac-STVHEILSKLSLEGY), both with their N-termini acetylated, were synthesized using standard Fmoc chemistry at the Penn State College of Medicine Macromolecular Core Facility. The AnI and AnII peptide sequences are the same sequences used by Rety et al. (14). In addition, a Tyr residue was introduced at the C-terminus of the AnII peptide to allow for quantification using UV absorbance spectroscopy. It is not expected that this residue would alter the binding specificity or affinity as it has been shown that it is the N-terminal region of the peptide which determines binding. In addition, in the crystal structure of the S100A10–AnII complex, the C-terminal region of the AnII peptide does not have well-defined electron density which suggests that that region of the peptide is not highly ordered which could also indicate that this region is not important for binding to S100A10 (14). The peptides were purified using C18 reverse phase HPLC using a 0 to 100% acetonitrile gradient in the presence of 30 mM ammonium acetate (pH 5.5) for AnI or in the presence of 0.065–0.05% TFA for AnII. The fractions containing peptide were subjected to three cycles of lyophilization and resuspension in Milli-Q water to remove residual TFA, or ammonium acetate. The molecular masses of the peptides were confirmed using MALDI-TOF and were found to be 1741.2 and 1717.7 Da for AnI and AnII, respectively. The molecular masses are in excellent agreement with the expected molecular masses of 1741.0 and 1717.9 Da for AnI and AnII, respectively, based on their amino acid compositions and N-terminal acetylation. Peptide concentrations were determined using the molar extinction coefficients at 280 nm (ϵ_{280}) of 5500 and 1490 M⁻¹ cm⁻¹ for AnI and AnII, respectively.

Analytical Equilibrium Ultracentrifugation. Analytical equilibrium ultracentrifugation experiments were performed on AnI and AnII to determine their oligomeric states using a Beckman XLA centrifuge at 4 °C and 35000 rpm in 20 mM Tris, 1 mM Tris (2-carboxyethyl)phosphine hydrochloride (TCEP), and 0.2 mM EDTA (pH 7.5) in the absence or presence of 5 mM calcium. The samples were considered to

be at equilibrium when there was no difference between three consecutive radial distribution scans, with 6 h between each scan. The data were fitted using nonlinear regression software (NLREG) to the following equation, which describes the radial distribution of a single species at equilibrium:

$$C_r = C_{r_0} \exp \left[\frac{\omega^2}{2RT} M(1 - \bar{v}\rho)(r^2 - r_0^2) \right] \quad (1)$$

where C_r is the peptide concentration at radius r , C_{r_0} is the concentration of monomeric peptide at r_0 , ω is the angular velocity, R is the gas constant equal to 8.134×10^7 erg mol⁻¹ K⁻¹, T is the temperature in kelvin, M is the monomer molecular mass, \bar{v} is the partial specific volume of the peptide [which is 0.748 and 0.745 cm³/g for AnI and AnII, respectively (17)], and ρ is the density of the solvent. From the fitted data, the molecular masses of AnI and AnII were found to be 1.9 ± 0.07 and 1.9 ± 0.16 kDa, respectively. These molecular masses are consistent with the ones expected from the amino acid composition of monomeric peptides.

Cloning of S100A6, S100A10, and S100A11. S100A6, S100A10, and S100A11 were cloned from Matched cDNA Pairs library (Clontech, Palo Alto, CA). The oligonucleotides used to PCR amplify the cDNA fragments for both proteins were based on their cDNA sequences complementary to the 5' and 3' ends. The PCR product for S100A10 was inserted into expression vector pGIA, using SphI and PstI restriction endonucleases, and the S100A6 and S100A11 cDNA was inserted into the pVEX expression vector, using the NdeI and PstI restriction endonucleases. Both pVEX and pGIA expression vectors are under the control of the T7 promoter and confer ampicillin resistance. Mutations on the S100A6 protein that introduce Y73F, Y84S, and Y73F/Y84S substitutions were made using the QuikChange approach. The DNA sequences were confirmed using an ABI 3130XL capillary sequencer.

Protein Purification. Sixteen representative members of the human S100 protein family (for S100 nomenclature used, see ref 18) (S100A1, S100A2, S100A3, S100A4, S100A5, S100A7, S100A8, S100A9, S100A12, S100A13, S100B, S100P, and S100Z) as well as calmodulin were expressed and purified as described previously (19–21). Protein expression was performed using *Escherichia coli* BL21(DE3) cells as protein expression is under the control of a T7 promoter. Cells were grown at 37 °C in 2×YT medium in the presence of 100 µg/mL ampicillin to an optical density at 600 nm of approximately 1 unit when isopropyl β-D-1-thiogalactopyranoside was added to a final concentration of 1 mM to induce protein expression. Protein expression was allowed to continue for 4 h at 37 °C and 225 rpm, after which the cells were harvested by centrifugation at 5000g and 4 °C for 40 min. The cells were resuspended in 50 mM Tris and 0.2 mM EDTA (pH 7.5) and stored at –20 °C. After thawing, the cells were lysed using a French pressure cell, after which 3 mM dithiothreitol (DTT) and 5 mM calcium were added, and the cellular debris was removed by centrifugation at 16000g and 4 °C for 45 min. The supernatant was loaded onto a Phenyl-Sepharose column equilibrated with 20 mM Tris, 0.2 mM EDTA, 5 mM calcium, and 3 mM DTT (pH 7.5) and washed with 15 column volumes of the same buffer to remove unbound proteins. Proteins were eluted using 20 mM Tris, 3 mM DTT, 5 mM

EGTA (pH 7.5) buffer, and fractions containing the protein of interest were passed through a Sephadex G-75 column equilibrated with 20 mM Tris, 0.2 mM EDTA, 5 mM calcium, and 3 mM DTT (pH 7.5). For S100A10, 8 M urea was used for elution instead of EGTA and the fractions containing the protein of interest were refolded by dialyzing the samples against 20 mM Tris, 3 mM DTT, 0.2 mM EDTA (pH 7.5) buffer, after which the protein was passed through a Sephadex G-75 column. The purity of the fractions containing the protein of interest was assessed using SDS-PAGE. In the cases where the protein of interest was not sufficiently pure, the samples were further purified using C18 reverse phase HPLC with a 0 to 100% acetonitrile gradient in the presence of 0.065–0.05% TFA and the purity was determined using SDS-PAGE. After the proteins were found to be pure (>95%), the proteins were dialyzed against double-deionized water with 0.001% ammonium hydroxide, lyophilized, and stored at -20°C .

Intrinsic Trp Fluorescence Experiments. Steady state fluorescence experiments were performed using a FluoroMax spectrofluorimeter. The AnI peptide contains a Trp residue which, on the basis of the crystal structure of the AnI–S100A11 complex, becomes buried in a hydrophobic region upon binding to S100A11 (15). Thus, changes in Trp fluorescence emission intensity and/or emission maximum can be used to monitor interactions between the AnI and S100 proteins. The experiments were performed at a constant temperature, 25°C , which was maintained using a thermostated cell holder and a circulating water bath. The buffer consisted of 20 mM Tris, 0.2 mM EDTA, and 3 mM DTT (pH 7.5), with 5 mM calcium (CaCl_2) or, as a control, without calcium. The Trp residue in AnI was selectively excited at 295 nm and the emission monitored from 305 to 400 nm. The initial concentration of AnI in the fluorescence cell was $2\ \mu\text{M}$. Small aliquots of concentrated protein solution, in the assay buffer, were added stepwise. The final concentration of protein was $10\ \mu\text{M}$, resulting in a final protein:peptide ratio of 5:1 at the end of titration. For the S100 proteins which contain Trp residues in their sequence (S100A1, S100A3, S100A8, S100A9, and S100A13), concentrated volumes of AnI were added to $2\ \mu\text{M}$ protein until the ratio of peptide to protein was 5:1. The titration data were corrected by subtracting the emission spectra for protein added to buffer, in the absence of peptide.

The molar extinction coefficients at 280 nm (ϵ_{280}) used to determine the protein concentrations were as follows: S100A1, $8480\ \text{M}^{-1}\text{cm}^{-1}$; S100A2, $2980\ \text{M}^{-1}\text{cm}^{-1}$; S100A3, $14440\ \text{M}^{-1}\text{cm}^{-1}$; S100A4, $2980\ \text{M}^{-1}\text{cm}^{-1}$; S100A5, $4470\ \text{M}^{-1}\text{cm}^{-1}$; S100A6, $4470\ \text{M}^{-1}\text{cm}^{-1}$; S100A7, $4470\ \text{M}^{-1}\text{cm}^{-1}$; S100A8, $11460\ \text{M}^{-1}\text{cm}^{-1}$; S100A9, $6990\ \text{M}^{-1}\text{cm}^{-1}$; S100A10, $2980\ \text{M}^{-1}\text{cm}^{-1}$; S100A11, $4470\ \text{M}^{-1}\text{cm}^{-1}$; S100A12, $2980\ \text{M}^{-1}\text{cm}^{-1}$; S100A13, $6990\ \text{M}^{-1}\text{cm}^{-1}$; S100B, $1490\ \text{M}^{-1}\text{cm}^{-1}$; S100P, $2980\ \text{M}^{-1}\text{cm}^{-1}$; S100Z, $2980\ \text{M}^{-1}\text{cm}^{-1}$; and calmodulin, $2980\ \text{M}^{-1}\text{cm}^{-1}$. These values were calculated as described in ref 22.

Far-UV Circular Dichroism. The far-UV CD spectra (260–200 nm) of free AnI and AnII were recorded on a Jasco-715 spectropolarimeter in a 1 mm light path length cuvette. Measurements were conducted under three different conditions. Buffer A consisted of 20 mM Tris, 3 mM DTT, and 0.2 mM EDTA (pH 7.5). Buffer B was the same as buffer A with additional 5 mM calcium. Buffer C was the

same as buffer B in the presence of 30% TFE. Peptide concentrations were $0.017\ \text{mg/mL}$, which corresponds to approximately $30\ \mu\text{M}$ for each peptide. The ellipticity values (Θ) for the peptides were corrected by subtracting the corresponding values for buffer only and converted to mean residue ellipticity, $[\Theta]$, using the following expression:

$$[\Theta] = \Theta \times \text{MR}/(10lc) \quad (2)$$

where MR is the mean molecular mass of the amino acids in each peptide (124 Da for AnI and 114 Da for AnII), l is the light path length in centimeters, and c is the peptide concentration in milligrams per milliliter. The fraction helicity, f_H , was determined as

$$f_H = \frac{[\Theta]_{222} - [\Theta]_C}{[\Theta]_H - [\Theta]_C} \quad (3)$$

where $[\Theta]_{222}$ is the experimentally determined ellipticity at 222 nm, $[\Theta]_C$ is the ellipticity of the fully coiled state, and $[\Theta]_H$ is the ellipticity of the fully helical state. The ellipticity of the fully coiled state, $[\Theta]_C$, has a temperature dependence described by (23)

$$[\Theta]_C = 640 - 45T \quad (4)$$

where T is the temperature in degrees Celsius. The ellipticity of the fully helical state, $[\Theta]_H$, for a protein or peptide consisting of N_r residues, has a temperature dependence described by (23)

$$[\Theta]_H = (-40000 + 250T) \left(1 - \frac{2.5}{N_r} \right) \quad (5)$$

To determine whether AnI and AnII form helical structures in the presence of their binding partners (i.e., S100A11, S100A10, and S100A6), far-UV CD spectra were recorded from 250 to 200 nm for $10\ \mu\text{M}$ protein in the presence of $50\ \mu\text{M}$ AnI or $50\ \mu\text{M}$ AnII, in binding buffer containing 5 mM calcium. The difference spectra, Θ_{diff} , were determined as follows:

$$\Theta_{\text{diff}} = \Theta_{\text{comp}} - (\Theta_{\text{pep}} + \Theta_{\text{prot}}) \quad (6)$$

where Θ_{comp} , Θ_{pep} , and Θ_{prot} are the ellipticities measured for the protein–peptide complex, free peptide, and free protein, respectively. Using eq 2, Θ_{diff} was converted to mean residue ellipticity assuming that the protein binding sites are saturated with bound peptide.

Isothermal Titration Calorimetry Experiments. Isothermal titration calorimetry (ITC) experiments were performed on a VP-ITC instrument (Microcal Inc., Northampton, MA) as described in refs 24 and 25. The ITC experiments were performed in 20 mM Tris, 0.2 mM EDTA, and 1 mM TCEP (pH 7.5) without calcium or with 5 mM calcium. To minimize differences in buffer composition, protein and peptide samples were dialyzed simultaneously with three buffer changes at 4°C . For the screening of binding between AnII and the S100 family members, as well as calmodulin, $2\ \mu\text{L}$ of approximately $0.75\ \text{mM}$ AnII was injected into the sample cell containing approximately $20\text{--}25\ \mu\text{M}$ protein. Since the heat of binding strongly depends on temperature, the experiments were performed at 10 and 25°C to ensure that the heat of binding can be observed. Heats of peptide

dilution were determined by performing injections of 2 μ L of peptide into buffer and were found to be insignificant. In cases where large heat effects, indicative of binding events, were observed, the titration was allowed to continue until saturation was achieved. In cases where no heat effect was observed, the titration was terminated after five injections.

ITC experiments were performed for the protein–peptide binding partners at five different temperatures. Due to limitations of AnI solubility, all titrations performed with AnI were performed by having the peptide in the cell and the protein in the syringe. Heats of dilution were <1% of the total heat when compared with that of a protein–peptide titration.

The heat of the reaction, Q , was obtained by integrating the peak after each injection of either peptide or protein into the cell, using scripts provided by the VP-ITC manufacturer (26). The heat of the reaction, after each injection, is related to the calorimetric enthalpy of binding, ΔH_{cal} , and the other thermodynamic parameters in a model-dependent way (26). For a homodimeric system, the two simplest models that were considered are as follows.

Two-identical binding sites model (per dimer):

$$Q = \frac{n[\text{cell}]_t \Delta H_{\text{cal}} V_o}{2} \left(A - \sqrt{A^2 - \frac{4[\text{syringe}]_t}{n[\text{cell}]_t}} \right) \quad (7)$$

where

$$A = 1 + \frac{[\text{syringe}]_t}{n[\text{cell}]_t} + \frac{[\text{syringe}]_t}{nK_a[\text{cell}]_t} \quad (8)$$

$n = 2$ is the stoichiometry of the peptide–protein complex, K_a is the association constant, $[\text{cell}]_t$ is the concentration of solute in the ITC cell with a volume V_o , and $[\text{syringe}]_t$ is the total concentration of injectant.

Two-sequential binding sites model (per dimer):

$$Q = [\text{cell}]_t V_o \{ [\Delta H_{\text{cal1}} K_1 [\text{syringe}]_t + (\Delta H_{\text{cal1}} + \Delta H_{\text{cal2}}) K_1 K_2 [\text{syringe}]_t^2] / [1 + [\text{syringe}]_t K_1 + 1 + K_1 K_2 [\text{syringe}]_t^2] \} \quad (9)$$

where K_1 and K_2 are the association constants for binding to sites 1 and 2, respectively, and ΔH_{cal1} and ΔH_{cal2} are the calorimetric enthalpies for binding to sites 1 and 2, respectively.

Structure-Based Calculation of ΔC_p . Structure-based calculation of thermodynamic parameters frequently allows validation of structural models (27). These calculations are usually based on changes in accessible surface area, ASA. To determine the total change in accessible surface upon binding ($\Delta \text{ASA}_{\text{tot}}$), the ASA of protein in the absence of peptide ($\text{ASA}_{\text{dim-pep}}$) and the ASA of unfolded peptide ($\text{ASA}_{\text{unf pep}}$) were subtracted from the ASA of the protein in complex with the peptide ($\text{ASA}_{\text{dim+pep}}$):

$$\Delta \text{ASA}_{\text{tot}} = \text{ASA}_{\text{dim+pep}} - (\text{ASA}_{\text{dim-pep}} + \text{ASA}_{\text{unf pep}}) \quad (10)$$

The changes in ΔASA were subdivided into aliphatic surface area, aromatic surface area, peptide backbone surface area, and polar surface area (28). The $\Delta \text{ASA}_{\text{tot}}$ was then converted into ΔC_p using the following relation (28):

$$\Delta C_p = 2.14 \Delta \text{ASA}_{\text{alp}} + 1.55 \Delta \text{ASA}_{\text{arm}} - 1.81 \Delta \text{ASA}_{\text{bb}} - 0.88 \Delta \text{ASA}_{\text{pol}} \quad (11)$$

where $\Delta \text{ASA}_{\text{alp}}$, $\Delta \text{ASA}_{\text{arm}}$, $\Delta \text{ASA}_{\text{pol}}$, and $\Delta \text{ASA}_{\text{bb}}$ are the changes in ASA for aliphatic amino acids, aromatic amino acids, polar amino acids, and the polypeptide backbone, respectively.

RESULTS AND DISCUSSION

Specificity of AnI or AnII Binding to S100 Family Members and Calmodulin. The AnI peptide, corresponding to the N-terminal sequence of annexin I, has been shown to bind with relatively high affinity to S100A11 (16, 29). Similarly, the AnII peptide, which corresponds to the N-terminal sequence of annexin II, was shown to bind S100A10 (15). The same group has also suggested that the interactions of AnI with S100A11 and AnII with S100A10 are specific (14). This conclusion was based on the observations that in their experiments no cross reactivity (i.e., of AnI with S100A10 and AnII with S100A11) was observed. However, a more recent report suggests that S100A11 does indeed interact with AnII (16). In this work, the binding specificity of the AnI and AnII peptides to 16 members of the S100 protein family (S100A1–S100A13, S100B, S100P, and S100Z) and calmodulin was investigated using intrinsic Trp fluorescence and/or isothermal titration calorimetry (ITC). Calmodulin has been included as a control for several reasons. It is a member of the EF-hand family and has four EF-hand motifs (30). It interacts with a rather diverse set of peptide sequences in a Ca^{2+} -dependent manner (27, 31). Upon binding to calmodulin, peptides adopt a helical conformation (2, 27, 31). It is known that at least one peptide, melittin, has the ability to bind both S100P (25) and calmodulin (27); however, these interactions seem to have little biological relevance. All these properties make calmodulin a relevant control in the context of this study addressing the issues of binding specificity of AnI and AnII peptides.

The fluorescence emission properties of tryptophan residues are a sensitive probe because they change depending on the polarity of the local environment. Trp residues which are highly exposed to polar environments (e.g., aqueous solution) have emission maxima in the range of 350–360 nm, whereas Trp residues in hydrophobic environments have emission maxima ranging between 330 and 345 nm (32). Figure 1A shows the fluorescence properties of the free AnI peptide in solution and of the AnI peptide in the presence of Ca^{2+} -S100A11. It can be seen that the fluorescence emission maximum wavelength shifts from approximately 359 nm for free AnI to 350 nm in the presence of Ca^{2+} -S100A11. The shift in emission maximum is also accompanied by a large increase in emission intensity, suggesting that the environment of the Trp residue on AnI becomes more hydrophobic. This observation is consistent with the crystal structure of the AnI– Ca^{2+} -S100A11 complex which shows that the Trp residue in AnI becomes buried in a hydrophobic environment upon binding (15). In the absence of calcium, there is very little change in the emission spectra, which is expected, as the S100A11–AnI interaction has been shown to be calcium-dependent (29). The dissociation constant, K_d , for the binding of AnI to Ca^{2+} -S100A11, determined using Trp fluorescence, was found to be 5 ± 1

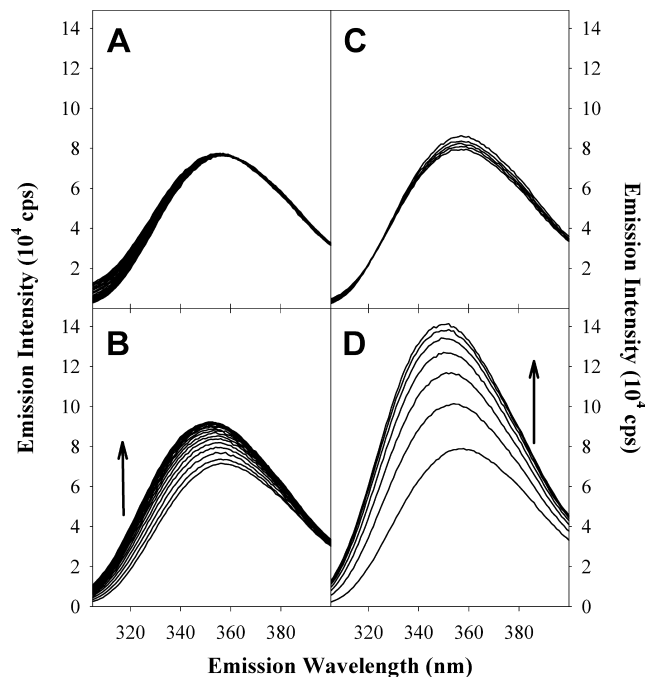


FIGURE 1: Changes in Trp fluorescence emission spectra at 25 °C of AnI for 1.2 μ M incremental additions of S100A11 in the absence of calcium (A) and in the presence of 5 mM calcium (B) and 1.2 μ M incremental additions of S100A6 in the absence of calcium (C) and in the presence of 5 mM calcium (D). The black arrows indicate the direction of the enhancement in Trp fluorescence emission for AnI in the presence of increasing concentrations of S100A11 or S100A6, which were taken to represent binding.

μ M (see Figure 2A) which is consistent with previous estimates (16). In addition, the K_d for the interaction of Ca^{2+} -S100A11 and AnI measured using Trp fluorescence is in excellent agreement with the K_d measured using ITC (see below), which validates the dual-method approach for detecting binding and determining the binding affinity.

Trp fluorescence was used to screen for binding of AnI to all 16 S100 protein family members and calmodulin (see Table S1 of the Supporting Information for a summary of the results). Addition of any other S100 proteins or calmodulin to AnI did not show changes in Trp fluorescence (i.e., emission maximum or emission intensity). Surprisingly, the only exception was found to be Ca^{2+} -S100A6. Figure 1B shows that AnI undergoes a large blue shift in its emission maximum wavelength, from approximately 359 to 352 nm, upon addition of Ca^{2+} -S100A6. The shift in emission maximum is also accompanied by a large increase in emission intensity. No changes in the Trp fluorescence of the AnI peptide, in the presence of S100A6, are observed if calcium is omitted from the binding buffer. Thus, addition of Ca^{2+} -S100A6 shows similar changes in the Trp fluorescence of AnI as the addition of Ca^{2+} -S100A11, suggesting that AnI also binds to the Ca^{2+} -S100A6 protein in a calcium-dependent manner. Interactions of AnI with the S100A6 protein have not been observed to date. Analysis of the titration profile (Figure 2B) yields a dissociation constant, K_d , for this interaction on the order of $17 \pm 4 \mu\text{M}$ which is 3-fold lower than the K_d for AnI binding to S100A11, $5 \pm 1 \mu\text{M}$.

The AnII peptide sequence does not contain any Trp residues, and only one Tyr residue. The fluorescence properties of Tyr are not as sensitive to its environment as those

of Trp. In addition, S100 proteins contain Tyr residues in their sequence, which also prevents the use of Tyr fluorescence spectroscopy for binding assays. As a result, the binding specificity of AnII with respect to all the members of the S100 protein family was determined using ITC, a method of choice for characterizing the thermodynamics of macromolecular interactions. A summary of the binding interactions of 16 S100 proteins and calmodulin with AnII as determined by ITC is given in Table S1 of the Supporting Information. It can be seen that AnII binds S100A10, which has been observed previously (14, 33). Moreover, the binding is independent of calcium, which is also consistent with previous findings that S100A10 does not have the ability to bind calcium and is locked in the ligand binding conformation (14).

Interestingly, in addition to binding S100A10, AnII is also found to bind Ca^{2+} -S100A11, and this binding to S100A11 is also modulated by calcium. The interaction between Ca^{2+} -S100A11 and AnII was initially shown not to occur (15). Recently, however, Rintala-Dempsey et al. (16) using NMR spectroscopy have shown that AnII can interact with Ca^{2+} -S100A11. A possible reason for the conflicting reports pertaining to the interaction between S100A11 and AnII is that Réty et al. (15) labeled AnII with Prodan, a fluorescent tag, which could have sterically hindered binding. In our work, and in the report by Rintala-Dempsey et al. (16), the AnII peptide was not modified by the addition of any extrinsic fluorescent probe.

In summary, AnI and AnII peptides were screened for interactions with 16 members of the S100 protein family and calmodulin. Neither peptide was found to bind to calmodulin, suggesting differences in specificity between the calmodulin and the S100 protein family. AnI has been found to bind Ca^{2+} -S100A6 and Ca^{2+} -S100A11, and AnII has been found to bind S100A10 and Ca^{2+} -S100A11. The observation that AnI and AnII each have a unique binding partner, i.e., S100A6 binding to AnI or S100A10 binding to AnII, and share a common binding partner, i.e., S100A11 binds both AnI and AnII, is quite remarkable. To gain a better understanding of these interactions, the binding between S100A11, S100A10, and S100A6 and AnI and AnII was further characterized using far-UV CD and isothermal titration calorimetry.

AnI and AnII Undergo a Coil–Helix Transition upon Binding. Far-UV circular dichroism (CD; from 250 to 190 nm) has been widely used to characterize the secondary structural content of proteins and peptides. A protein, or peptide, with a high level of helical structure would have a CD spectrum with characteristic minima at 222 and 208 nm, whereas a spectrum corresponding to a β -sheet has a minimum at approximately 215 nm (34). Unstructured polypeptides tend to have far-UV CD spectra lacking the aforementioned features. Far-UV CD spectra of free AnI and AnII were recorded in the absence and presence of calcium to determine whether they are structured and whether the presence of calcium has an effect on their secondary structure (data not shown). The helical propensities of the AnI and AnII peptides according to AGADIR (35) are expected to be relatively low, $<2\%$. Indeed, the experimentally measured far-UV CD spectra of AnI and AnII do not show the characteristic minima for either α -helices or β -sheets. Thus, we can conclude that AnI and AnII are both devoid of regular

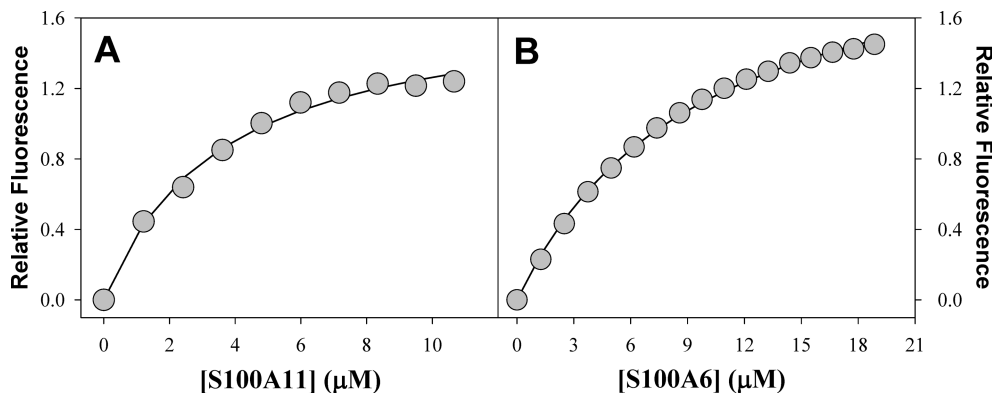


FIGURE 2: Changes in intrinsic Trp fluorescence of AnI as a function of the concentration of Ca²⁺-S100A11 (A) and Ca²⁺-S100A6 (B). The symbols represent the experimental values and the solid lines represent the fits of the experimental data to eq 7. The dissociation constants for the binding of AnI to S100A11 and S100A6 were found to be 5 ± 1 and 17 ± 4 μM, respectively.

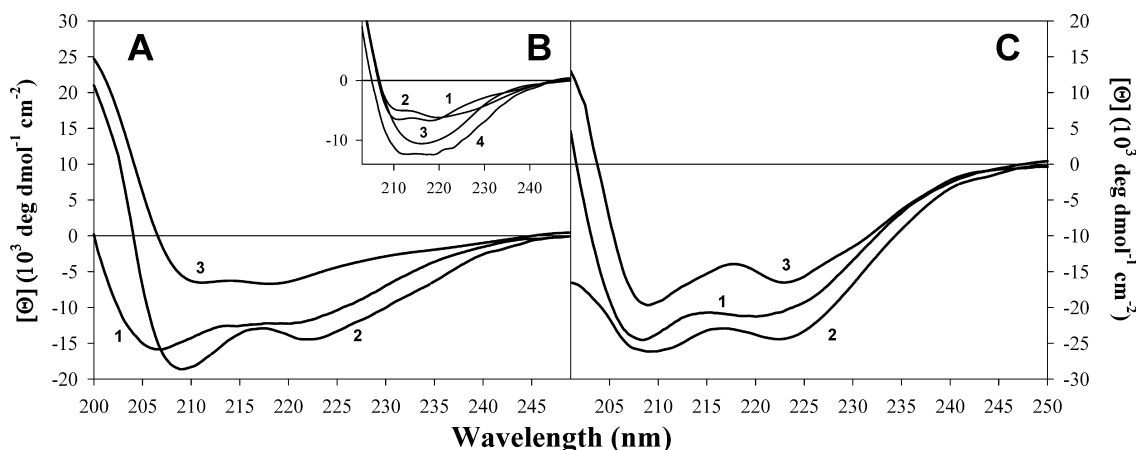


FIGURE 3: Far-UV CD difference spectra for AnI and AnII binding to their respective S100 protein binding partners, in the presence of 5 mM calcium, determined using eq 6. Panel A shows the far-UV CD spectrum for AnI in 60% TFE (curve 1; shown for comparison) and the difference spectra for AnI bound to S100A11 (curve 2) and for AnI bound to wild-type S100A6 (curve 3). Panel B shows the difference spectra for AnI bound to wild-type S100A6 (curve 1; shown for comparison), S100A6-Y84S (curve 2), S100A6-Y73F (curve 3), and S100A6-Y73F/Y84S (curve 4). Panel C shows the far-UV CD spectrum for AnII in the presence of 60% TFE (curve 1; shown for comparison) and the far-UV CD difference spectra for AnII bound to S100A10 (curve 2) and S100A11 (curve 3).

secondary structure in solution. To determine the potential for helix formation by AnI and AnII, trifluoroethanol (TFE) was added to each peptide up to a final concentration of 60%, in the presence and absence of calcium. It is well-known that TFE promotes helix formation for peptides which are devoid of regular secondary structure (36). In the presence of TFE, both AnI and AnII have far-UV CD spectra characteristic of helices, which are similar irrespective of whether calcium is present (see Figure 3). Taken together, these results show that even though the intrinsic helical propensities of AnI and AnII in aqueous solution are low, they can form helices in the presence of TFE.

It is well established that AnI and AnII adopt helical conformations when bound to Ca²⁺-S100A11 and S100A10, respectively [Protein Data Bank (PDB) entries 1QLS (15) and 1BT6 (14)]. It is, however, not known whether AnI and AnII undergo the same conformational change upon binding to Ca²⁺-S100A6 and Ca²⁺-S100A11, respectively. For this reason, the far-UV CD spectra of peptides in the presence of the corresponding S100 proteins (i.e., AnI in the presence of Ca²⁺-S100A6 and Ca²⁺-S100A11 and AnII in the presence of S100A10 and Ca²⁺-S100A11) were recorded. Figure 3 shows the difference far-UV CD spectra for all the binding partners.

It can be observed that in most cases the peptides form helices upon binding to their respective binding partners. A noted lower ellipticity is observed for the far-UV CD spectrum for AnI binding to Ca²⁺-S100A6. There are two possible explanations for this. First, it is possible that AnI forms a more extensive helix when binding to S100A11 than it does when binding to S100A6. Second, the unusual far-UV CD spectrum could be due to the contribution of aromatic side chains to the measured CD spectrum. Chakrabarty et al. (37) have shown that aromatic amino acids, Tyr and Trp, have opposite effects on far-UV CD spectra of peptides. They have shown that the difference spectrum for a peptide containing a Tyr residue has a positive Cotton effect (i.e., leading to an apparent decrease in helical content) whereas a Trp-containing peptide has a negative Cotton effect (i.e., leading to an overestimate of helical content). The fact that both AnI and AnII have the same difference spectra when binding Ca²⁺-S100A11, with fractional helicities of 0.59 and 0.57, respectively, supports the argument that it is the environment on the binding surface of Ca²⁺-S100A6 which could be responsible for the observation made with AnI and the S100A6 complex. On the basis of the sequence comparison of S100A11 and S100A6 (Figure 4), there are two additional Tyr residues in the sequence of S100A6 (at positions 73 and 84) that are Phe and Cys, respectively, in

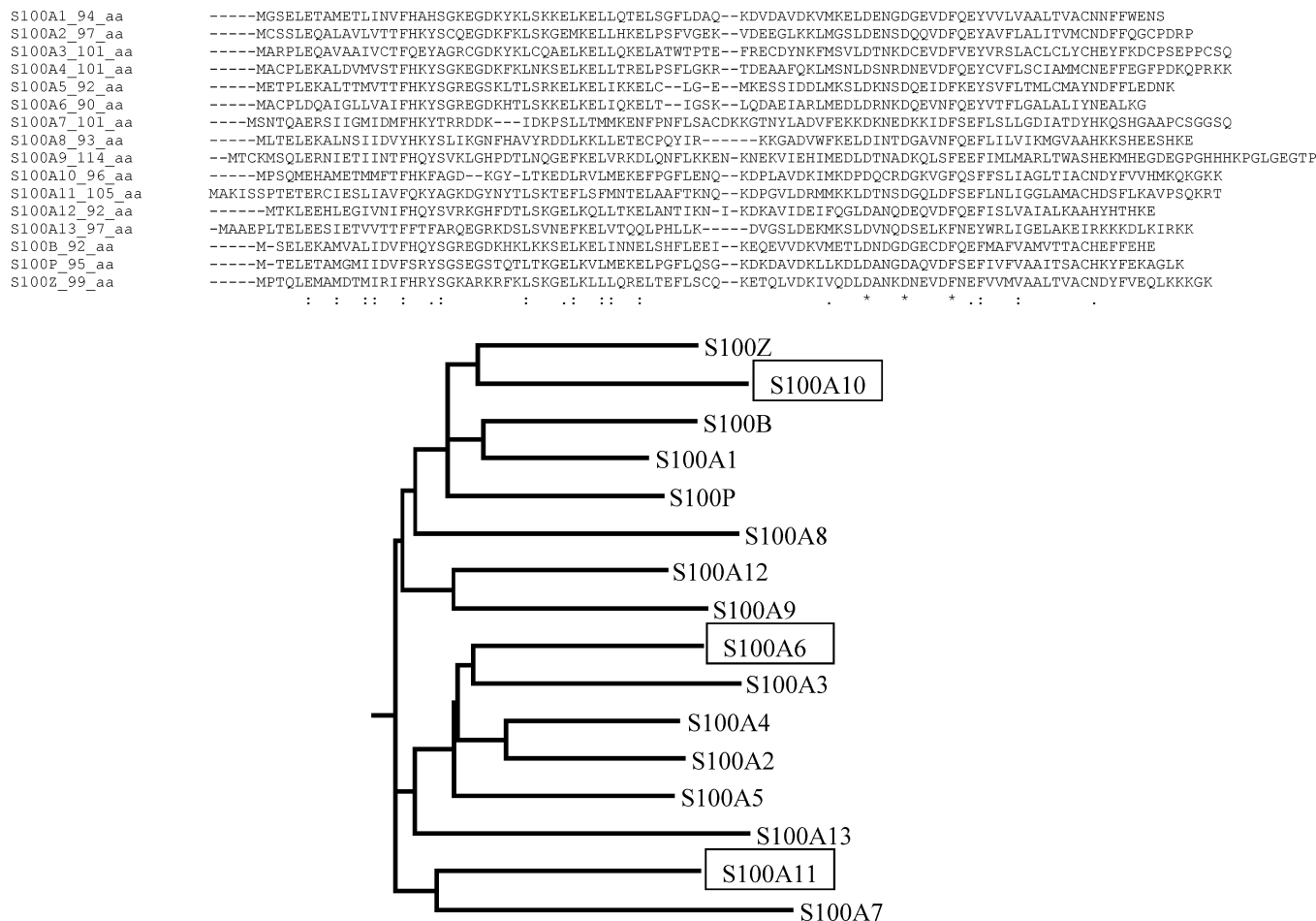


FIGURE 4: Sequence alignment of human S100 family members generated using ClustalW. Also shown is the phylogenetic tree based on the sequence alignment. For the sake of clarity, S100A6, S100A10, and S100A11 are highlighted in the phylogenetic tree.

S100A11. It is possible that upon peptide binding, the environments of the Tyr residues change leading to a positive Cotton effect which could decrease the overall far-UV CD spectrum. Consequently, this could mask the characteristic helical far-UV CD spectrum for the bound peptide. To test this hypothesis, Tyr73 and Tyr84 in S100A6 were substituted with Phe and Ser, respectively. The Tyr84 was substituted with Ser and not Cys, as found in S100A11, so as to avoid possible disulfide bond formation. It appears that Y73F contributes to the apparent lower intensity of far-UV CD. This can be seen from the comparison of far-UV CD spectrum of AnI upon binding to the wild type, Y73F, Y84S or Y73F/Y84S variants of S100A6. Indeed, the difference spectrum for the Y84S variant has a similar spectrum to that of the wild type, while the difference spectra for Y73F and Y73F/Y84S are similar to that of the difference far-UV CD spectrum of AnI upon binding to S100A11 or AnI in 60% TFE. Importantly, the substitutions do not have a significant effect on the binding affinity (data not shown). These results support the notion that both AnI and AnII peptides undergo a coil-to-helix transition upon binding to Ca^{2+} -S100A6 and Ca^{2+} -S100A11 or S100A10 and Ca^{2+} -S100A11, respectively.

Thermodynamics of Peptide Binding. From the Trp fluorescence and ITC screening results, as well as the far-UV CD results, it has been shown that Ca^{2+} -S100A6 and Ca^{2+} -S100A11 bind AnI whereas S100A10 and Ca^{2+} -S100A11 bind AnII. The thermodynamics of these interactions were further characterized in detail by performing ITC experiments at different temperatures. ITC, in many cases,

is the method of choice for measuring the thermodynamics of protein–protein interactions. It simultaneously provides the estimates for the binding constant (and thus the Gibbs energy of binding), the enthalpy of binding, and the stoichiometry of binding. A drawback of ITC, however, is that the analysis of the data is model-dependent.

Figure 5A shows an example of an ITC experiment in which Ca^{2+} -S100A11 was titrated into AnI. The ITC titration data were best fit to the simplest model, two identical noninteracting binding sites per dimer of Ca^{2+} -S100A11, described by eq 7. This model is essentially equivalent to a model with one peptide binding site per Ca^{2+} -S100A11 monomer (see Table 1 for a summary of the thermodynamic data). The K_d per binding site for the interaction of Ca^{2+} -S100A11 with AnI was found to be $5 \pm 2 \mu\text{M}$ which is in excellent agreement with the K_d of $5 \pm 1 \mu\text{M}$ determined using Trp fluorescence. ITC experiments were performed for the temperature range from 15 to 35 °C. Figure 6 shows the dependence of the enthalpy of binding, ΔH_{cal} , on temperature. The enthalpy of binding of AnI to Ca^{2+} -S100A11 is always negative and decreases with an increase in temperature from -4 kJ/mol at 15 °C to -30 kJ/mol at 35 °C. At the same time, the equilibrium dissociation constant does not depend significantly on temperature (see Table S2 of the Supporting Information), leading to a weak temperature dependence of the free energy of binding [$\Delta G = -RT \ln(K_d) \approx 30 \text{ kJ/mol}$, per binding site]. This suggests that the binding of AnI to Ca^{2+} -S100A11 is entropically driven.

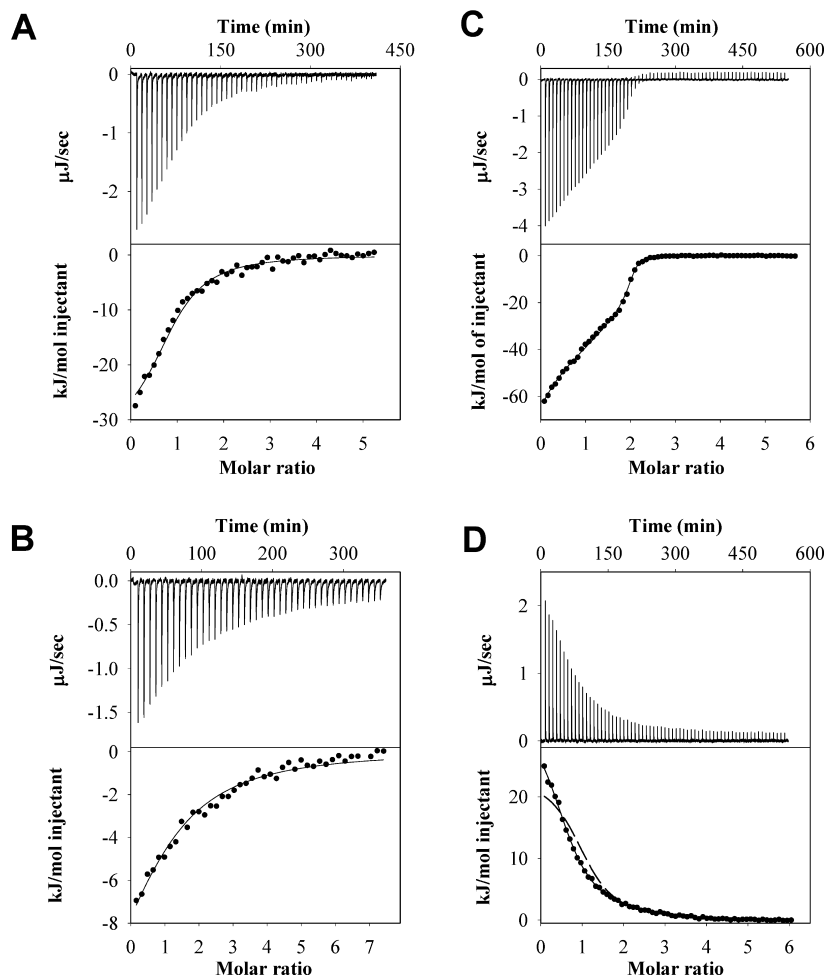


FIGURE 5: Examples of ITC experiments for AnI or AnII binding to their specific S100 protein binding partners. Shown for each example are the heat effects (microjoules per second) as a function of time, the cumulative heat effects (kilojoules per mole and represented by symbols) as a function of the molar ratio of peptide to protein, and the fits to the experimental data (solid lines) for AnI binding to S100A11 at 35 °C (A; data fitted to eq 7), AnI binding to S100A6 at 35 °C (B; data fitted to eq 7), AnII binding to S100A10 at 15 °C (C; data fitted to eq 9), and AnII binding to S100A11 at 6 °C (D; data fitted to eq 9). For the sake of comparison, the dashed line in panel D shows the experimental binding data fitted to a model describing identical binding sites (eq 7).

Table 1: Summary of the Thermodynamic Properties of S100A6, S100A10, and S100A11 Binding to AnI and AnII Determined Using Trp Fluorescence Titrations and ITC Experiments as Well as a Comparison with Structure-Based Calculations

protein	AnI K_d (μ M)	AnII K_{d1} and K_{d2} (μ M)	AnI $\Delta C_{p,exp}$ ($\text{kJ mol}^{-1} \text{K}^{-1}$)	AnI $\Delta C_{p,calc}$ ($\text{kJ mol}^{-1} \text{K}^{-1}$)	AnII $\Delta C_{p,exp}$ ($\text{kJ mol}^{-1} \text{K}^{-1}$)	AnII $\Delta C_{p,calc}$ ($\text{kJ mol}^{-1} \text{K}^{-1}$)
S100A6	13 ± 4 (17 ± 4) ^a		-1.1 ± 0.3	-1.6 ± 0.5		
S100A11	5 ± 2 (5 ± 1) ^a		-1.3 ± 0.2	-1.5 ± 0.3		
S100A11		1.7 ± 1.2 and 9.2 ± 1.9			-1.1 ± 0.2	-1.4 ± 0.3
S100A10		0.5 ± 0.4 and 0.5 ± 0.3			-2.4 ± 0.3	-1.7 ± 0.3

^a Values in parentheses were determined using Trp fluorescence.

The binding of AnI to Ca^{2+} -S100A6 is a novel interaction, which was identified by us using Trp fluorescence and was further confirmed using ITC. Figure 5B shows an example of an ITC experiment in which Ca^{2+} -S100A6 was titrated into AnI. The data were best fit to a model with two identical noninteracting binding sites per dimer of Ca^{2+} -S100A6 described by eq 7. The K_d for the interaction was found to be $13 \pm 4 \mu\text{M}$ (see Table 1 for a summary of the thermodynamic parameters). This compares well with the K_d of $17 \pm 4 \mu\text{M}$ for AnI binding to Ca^{2+} -S100A6 determined using Trp fluorescence to monitor the binding (Figure 2B). It is also comparable to the K_d of $5 \pm 1 \mu\text{M}$ for AnI binding to Ca^{2+} -S100A11 determined from Trp fluorescence titration experiments (Figure 2A) and ITC (Figure 5). The similarity in the thermodynamics of binding of the

AnI peptide to Ca^{2+} -S100A11 and Ca^{2+} -S100A6 extends beyond the similarities in K_d values. Figure 6 compares the enthalpies of binding of AnI to Ca^{2+} -S100A11 and Ca^{2+} -S100A6 at different temperatures. The enthalpies of binding are either negative or positive but small relative to the free energy of binding [$\Delta G = -RT \ln(K_d) \approx 26$ or 30 kJ/mol , per binding site, for AnI binding to Ca^{2+} -S100A11 or Ca^{2+} -S100A6, respectively]. This suggests that binding of AnI to both these proteins is entropically driven. The other remarkable similarity for thermodynamics of binding of AnI to Ca^{2+} -S100A11 and Ca^{2+} -S100A6 is that both have similar slopes for ΔH_{cal} dependencies on temperature, -1.3 ± 0.2 and $-1.1 \pm 0.2 \text{ kJ mol}^{-1} \text{K}^{-1}$, respectively. The slope of the ΔH_{cal} dependence on temperature represents the heat capacity changes upon binding, ΔC_p . The values of ΔC_p for

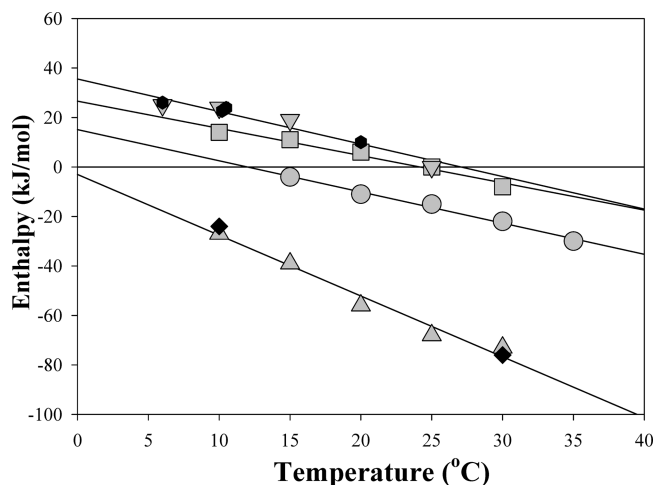


FIGURE 6: Temperature dependence of the enthalpies, ΔH_{cal} , of AnI and AnII binding to their specific S100 protein binding partners: AnII binding to S100A10 in the presence of 5 mM calcium (▲) and in the absence of calcium (▼), AnII binding to S100A11 in the absence of NaCl (▼) and in the presence of 100 mM NaCl (●), AnI binding to S100A11 (■), and AnI binding to S100A6 (●). Solid lines represent linear fits of the ΔH_{cal} temperature dependencies for each S100–peptide interaction. The slopes of these lines represent the changes in heat capacity, which are summarized in Table 1.

protein–protein interactions can be calculated from the structural information for the interacting proteins before and after complex formation (see Materials and Methods for details). Using the structure of AnI in complex with Ca^{2+} -S100A11, determined by X-ray crystallography (15), and the approach described in Materials and Methods (see eqs 10 and 11), the change in ΔC_p for AnI binding to Ca^{2+} -S100A11 is predicted to be $-1.5 \pm 0.3 \text{ kJ mol}^{-1} \text{ K}^{-1}$ which is in very good agreement with the experimentally measured values (see Table 1).

There are currently no structures available for the AnI peptide bound to Ca^{2+} -S100A6 as this is the first description of this interaction. There is, however, ample evidence that this complex is probably structurally similar to the AnI- Ca^{2+} -S100A11 complex (15). Consequently, the structure of the complex was modeled by threading the S100A6 sequence into the structure of S100A11 or threading the sequence of AnI into the structure of the Ca^{2+} -S100A6 complex with another unrelated peptide (38). It was found that the experimentally determined ΔC_p ($-1.1 \pm 0.2 \text{ kJ mol}^{-1} \text{ K}^{-1}$) and the expected ΔC_p ($-1.6 \pm 0.5 \text{ kJ mol}^{-1} \text{ K}^{-1}$) are in relatively good agreement, taking into consideration the fact that the AnI- Ca^{2+} -S100A6 complex is a homology model. This correspondence of the calculated and experimental values of ΔC_p for AnI binding to Ca^{2+} -S100A6, together with the CD data (see Figure 3), provides strong support for the similarity of the mode of binding of AnI to these two distinctive proteins, S100A6 and S100A11.

Figure 5C shows a representative ITC profile for the titration of AnII into S100A10. The binding isotherm cannot be fit to the simplest model (two identical noninteracting binding sites per dimer of S100A10) represented by eq 7 because of its clear biphasic shape. Since ITC data analysis is model-dependent and should therefore follow the principle of Occam's Razor, the next simplest model could be one that has two nonidentical noninteracting binding sites. However, this model cannot hold true due to the symmetry

of the S100A10 homodimer. Thus, the binding isotherm was fitted to a model that assumes two sequential binding sites per S100A10 dimer. The fit to this model is very good not only at 15 °C (shown in Figure 5B) but also at all other temperatures and solvent conditions (data not shown). The dissociation constants from the fit are summarized in Table 1. The implication of this model is that one of the two sites of the S100A10 homodimer must be occupied before the other. Such an order of binding events is possibly due to the fact that there are several interactions made with the peptide from both subunits of the homodimer. The interactions formed upon binding the first peptide are transduced through a slight adjustment of the dimer interface onto the other subunit of the S100A10 homodimer, resulting in enhanced binding at the second binding site.

Figure 6 shows the plot of ΔH_{cal} , the total enthalpy from both binding sites, versus temperature. It is remarkable that the enthalpy is large and negative for the entire range of temperatures, again suggesting that AnII binding to S100A10 is entropically driven. This entropically driven binding of AnI to Ca^{2+} -S100A6 and Ca^{2+} -S100A11; however, in these latter two cases, the binding is modulated by calcium ions. S100A10 is an exception among all other S100 proteins in that it does not bind calcium or any other divalent ions (14). It has been suggested that S100A10 is “locked” in the ligand-binding-competent state. Consequently, it is expected that the binding of AnII to S100A10 should be independent of calcium as S100A10 does not have the ability to bind calcium. Indeed, the ITC experiments for binding of AnII to S100A10 performed in the presence of calcium are very similar to the data obtained in the absence of calcium (see Figure 6), suggesting that the entropically driven peptide binding to these S100 proteins is not related to calcium binding.

The temperature dependence of the enthalpy of AnII binding to S100A10 is very similar to the ΔC_p observed previously for the peptide melittin binding to Ca^{2+} -S100P (25). For the latter system, the ΔC_p was estimated to be $-2.5 \pm 0.5 \text{ kJ mol}^{-1} \text{ K}^{-1}$ which compares well with the ΔC_p of $-2.4 \pm 0.3 \text{ kJ mol}^{-1} \text{ K}^{-1}$ for AnII binding to S100A10. Interestingly, in both cases, the values for ΔC_p predicted from structure-based calculations according to eq 11 gave estimates ($-1.7 \text{ kJ mol}^{-1} \text{ K}^{-1}$) similar to albeit lower than the experimentally measured ΔC_p (Figure 6).

Even though it was initially shown that Ca^{2+} -S100A11 and AnII do not interact (14), recent NMR experiments suggest that there is an interaction (16). By screening for interactions of S100 proteins with AnII using ITC, we found independently that S100A11 indeed does bind the AnII. The enthalpy of binding of AnII to Ca^{2+} -S100A11 is endothermic, while the enthalpy of AnII binding to S100A10 is exothermic. To further investigate these differences in sign of heat effects, ITC experiments for AnII binding to Ca^{2+} -S100A11 were performed in 100 mM NaCl. The higher ionic strength, however, did not have any effect on the thermodynamics of binding (see, e.g., Figure 6), thus eliminating the possibility that this is a nonspecific electrostatically driven interaction. ITC titration data cannot be fit to the simplest model, two identical noninteracting binding sites per dimer of Ca^{2+} -S100A11, represented by eq 7 (see Figure 5D). However, as for the AnII–S100A10 ITC titration profile, the ITC data

can be fit well to a model that assumes two sequential binding sites for AnII per Ca^{2+} -S100A11 dimer (see Figure 5D). The dissociation constants for this model were found to be 2 ± 1 and $9 \pm 2 \mu\text{M}$. As in the case of AnII-S100A10 interactions, the two-sequential binding sites model that describes best the AnII- Ca^{2+} -S100A11 interactions suggests a thermodynamic linkage between binding sites.

The enthalpy of interaction between AnII and Ca^{2+} -S100A11 is endothermic but small relative to the Gibbs energy of binding, indicating that as in all previous cases binding is entropically driven. This entropically driven binding is observed at all studied temperatures. This is despite the fact that the enthalpy of interactions is strongly temperature dependent with an experimentally determined ΔC_p of $-1.1 \text{ kJ mol}^{-1} \text{ K}^{-1}$, a value very similar to that of $-1.4 \text{ kJ mol}^{-1} \text{ K}^{-1}$ calculated from the modeled structure of the AnII complex with Ca^{2+} -S100A11 (using eq 11). Such good correspondence between calculated and experimental values of ΔC_p implies that there are sufficient degrees of similarities in the structures that can be predicted by homology modeling. Despite this, it is not sufficient to explain, for example, why and how AnII becomes more helical when bound to S100A10 compared to when it is bound to S100A11 or to explain why AnI and AnII peptides bind to only these S100 proteins and not the others.

CONCLUSIONS

By screening for binding for AnI and AnII against representatives of the human S100 protein family under defined conditions, we have shown that very few members of the protein family bind the two peptides. This suggests that the observed binding interactions are specific. In addition to demonstrating this specificity, we also confirmed the recently suggested interaction between AnII and Ca^{2+} -S100A11. Furthermore, we have identified a novel interaction between Ca^{2+} -S100A6 and AnI. These interactions, as suggested previously, are modulated by calcium. Detailed thermodynamic and spectroscopic characterization of the interactions revealed additional common properties. First, binding in all four studied pairs of interacting partners is entropically driven. Second, both AnI and AnII peptides, unstructured when free in solution, fold into a helical conformation upon binding.

The exact cellular functions of the S100 proteins are not known even though there are several reports identifying different target proteins. One of the main limitations of the approaches used to screen for potential S100 interacting partners is that the target protein with the highest binding affinity would be identified. This could lead to only a single target protein being identified as interacting with the specific S100 protein family member, which would suggest that the interaction is specific. The overlap in binding specificity observed here could provide a reason for why gene knockout approaches to mapping the function of S100 proteins have not led to an identifiable phenotypic change (see ref 3 for examples). The response to changing cellular calcium levels is critical to the survival of the cells, and it is therefore not unexpected that the functionality of the S100 proteins could overlap.

SUPPORTING INFORMATION AVAILABLE

Summary of interactions of AnI and AnII with S100 protein family members (Table S1) and thermodynamic parameters determined using ITC for AnI and AnII binding to their respective S100 protein binding partners (Table S2). This material is available free of charge via the Internet at <http://pubs.acs.org>.

REFERENCES

1. Santamaria-Kisiel, L., Rintala-Dempsey, A. C., and Shaw, G. S. (2006) Calcium-dependent and -independent interactions of the S100 protein family. *Biochem. J.* 396, 201–214.
2. Bhattacharya, S., Bunick, C. G., and Chazin, W. J. (2004) Target selectivity in EF-hand calcium binding proteins. *Biochim. Biophys. Acta* 1742, 69–79.
3. Marenholz, I., Heizmann, C. W., and Fritz, G. (2004) S100 proteins in mouse and man: From evolution to function and pathology (including an update of the nomenclature). *Biochem. Biophys. Res. Commun.* 322, 1111–1122.
4. Zimmer, D. B., Wright Sadosky, P., and Weber, D. J. (2003) Molecular mechanisms of S100-target protein interactions. *Microsc. Res. Tech.* 60, 552–559.
5. Rintala-Dempsey, A. C., Rezvanpour, A., and Shaw, G. S. (2008) S100-annexin complexes: Structural insights. *FEBS J.* (in press).
6. Donato, R. (2003) Intracellular and extracellular roles of S100 proteins. *Microsc. Res. Tech.* 60, 540–551.
7. Ghavami, S., Kerkhoff, C., Chazin, W. J., Kadkhoda, K., Xiao, W., Zuse, A., Hashemi, M., Eshraghi, M., Schulze-Osthoff, K., Klonisch, T., and Los, M. (2008) S100A8/9 induces cell death via a novel, RAGE-independent pathway that involves selective release of Smac/DIABLO and Omi/HtrA2. *Biochim. Biophys. Acta* 1783, 297–311.
8. Wilder, P. T., Lin, J., Bair, C. L., Charpentier, T. H., Yang, D., Liriano, M., Varney, K. M., Lee, A., Oppenheim, A. B., Adhya, S., Carrier, F., and Weber, D. J. (2006) Recognition of the tumor suppressor protein p53 and other protein targets by the calcium-binding protein S100B. *Biochim. Biophys. Acta* 1763, 1284–1297.
9. Heizmann, C. W., and Cox, J. A. (1998) New perspectives on S100 proteins: A multi-functional Ca^{2+} , Zn^{2+} - and Cu^{2+} -binding protein family. *BioMetals* 11, 383–397.
10. Ravasi, T., Hsu, K., Goyette, J., Schroder, K., Yang, Z., Rahimi, F., Miranda, L. P., Alewood, P. F., Hume, D. A., and Geczy, C. (2004) Probing the S100 protein family through genomic and functional analysis. *Genomics* 84, 10–22.
11. Ivanenkov, V. V., Jamieson, G. A., Jr., Gruenstein, E., and Dimlich, R. V. (1995) Characterization of S-100b binding epitopes. Identification of a novel target, the actin capping protein, CapZ. *J. Biol. Chem.* 270, 14651–14658.
12. Rustandi, R. R., Drohat, A. C., Baldissari, D. M., Wilder, P. T., and Weber, D. J. (1998) The Ca^{2+} -dependent interaction of S100B($\beta\beta$) with a peptide derived from p53. *Biochemistry* 37, 1951–1960.
13. Bhattacharya, S., Large, E., Heizmann, C. W., Hemmings, B., and Chazin, W. J. (2003) Structure of the Ca^{2+} /S100B/NDR kinase peptide complex: Insights into S100 target specificity and activation of the kinase. *Biochemistry* 42, 14416–14426.
14. Rety, S., Sopkova, J., Renouard, M., Osterloh, D., Gerke, V., Tabaries, S., Russo-Marie, F., and Lewit-Bentley, A. (1999) The crystal structure of a complex of p11 with the annexin II N-terminal peptide. *Nat. Struct. Biol.* 6, 89–95.
15. Rety, S., Osterloh, D., Arie, J. P., Tabaries, S., Seeman, J., Russo-Marie, F., Gerke, V., and Lewit-Bentley, A. (2000) Structural basis of the Ca^{2+} -dependent association between S100C (S100A11) and its target, the N-terminal part of annexin I. *Structure* 8, 175–184.
16. Rintala-Dempsey, A. C., Santamaria-Kisiel, L., Liao, Y., Lajoie, G., and Shaw, G. S. (2006) Insights into S100 target specificity examined by a new interaction between S100A11 and annexin A2. *Biochemistry* 45, 14695–14705.
17. Makhatadze, G. I., Medvedkin, V. N., and Privalov, P. L. (1990) Partial molar volumes of polypeptides and their constituent groups in aqueous solution over a broad temperature range. *Biopolymers* 30, 1001–1010.
18. Marenholz, I., Lovering, R. C., and Heizmann, C. W. (2006) An update of the S100 nomenclature. *Biochim. Biophys. Acta* 1763, 1282–1283.

19. Gribenko, A., Lopez, M. M., Richardson, J. M., III., and Makhatadze, G. I. (1998) Cloning, overexpression, purification, and spectroscopic characterization of human S100P. *Protein Sci.* 7, 211–215.
20. Gopalakrishna, R., and Anderson, W. B. (1982) Ca²⁺-induced hydrophobic site on calmodulin: Application for purification of calmodulin by phenyl-Sepharose affinity chromatography. *Biochem. Biophys. Res. Commun.* 104, 830–836.
21. Gribenko, A. V., Hopper, J. E., and Makhatadze, G. I. (2001) Molecular characterization and tissue distribution of a novel member of the S100 family of EF-hand proteins. *Biochemistry* 40, 15538–15548.
22. Gill, S. C., and von Hippel, P. H. (1989) Calculation of protein extinction coefficients from amino acid sequence data. *Anal. Biochem.* 182, 319–326.
23. Rohl, C. A., and Baldwin, R. L. (1998) Deciphering rules of helix stability in peptides. *Methods Enzymol.* 295, 1–26.
24. Lopez, M. M., and Makhatadze, G. I. (2002) Isothermal titration calorimetry. *Methods Mol. Biol.* 173, 121–126.
25. Gribenko, A. V., Guzman-Casado, M., Lopez, M. M., and Makhatadze, G. I. (2002) Conformational and thermodynamic properties of peptide binding to the human S100P protein. *Protein Sci.* 11, 1367–1375.
26. Wiseman, T., Williston, S., Brandts, J. F., and Lin, L. N. (1989) Rapid measurement of binding constants and heats of binding using a new titration calorimeter. *Anal. Biochem.* 179, 131–137.
27. Brokx, R. D., Lopez, M. M., Vogel, H. J., and Makhatadze, G. I. (2001) Energetics of target peptide binding by calmodulin reveals different modes of binding. *J. Biol. Chem.* 276, 14083–14091.
28. Makhatadze, G. I., and Privalov, P. L. (1995) Energetics of protein structure. *Adv. Protein Chem.* 47, 307–425.
29. Mailliard, W. S., Haigler, H. T., and Schlaepfer, D. D. (1996) Calcium-dependent binding of S100C to the N-terminal domain of annexin I. *J. Biol. Chem.* 271, 719–725.
30. Babu, Y. S., Bugg, C. E., and Cook, W. J. (1988) Structure of calmodulin refined at 2.2 Å resolution. *J. Mol. Biol.* 204, 191–204.
31. Clore, G. M., Bax, A., Ikura, M., and Gronenborn, A. M. (1993) Structure of Calmodulin Target Peptide Complexes. *Curr. Opin. Struct. Biol.* 3, 838–845.
32. Lakowicz, J. R. (2006) *Principles of Fluorescence Spectroscopy*, 3rd ed., Springer, New York.
33. Becker, T., Weber, K., and Johnsson, N. (1990) Protein-protein recognition via short amphiphilic helices: A mutational analysis of the binding site of annexin II for p11. *EMBO J.* 9, 4207–4213.
34. Johnson, W. C., Jr. (1990) Protein secondary structure and circular dichroism: A practical guide. *Proteins* 7, 205–214.
35. Lacroix, E., Viguera, A. R., and Serrano, L. (1998) Elucidating the folding problem of α -helices: Local motifs, long-range electrostatics, ionic-strength dependence and prediction of NMR parameters. *J. Mol. Biol.* 284, 173–191.
36. Nelson, J. W., and Kallenbach, N. R. (1986) Stabilization of the ribonuclease S-peptide α helix by trifluoroethanol. *Proteins* 1, 211–217.
37. Chakrabartty, A., Kortemme, T., Padmanabhan, S., and Baldwin, R. L. (1993) Aromatic side-chain contribution to far-ultraviolet circular dichroism of helical peptides and its effect on measurement of helix propensities. *Biochemistry* 32, 5560–5565.
38. Lee, Y. T., Dimitrova, Y. N., Schneider, G., Ridenour, W. B., Bhattacharya, S., Soss, S. E., Caprioli, R. M., Filipek, A., and Chazin, W. J. (2008) Structure of the S100A6 Complex with a Fragment from the C-Terminal Domain of Siah-1 Interacting Protein: A Novel Mode for S100 Protein Target Recognition. *Biochemistry* 47, 10921–10932.

BI8019959